Low Vibration Sensitivity MEMS Resonators

Kenneth E. Wojciechowski, Roy H. Olsson III, Michael S. Baker, Jonathan W. Wittwer
Kevin J. Smart, James G. Fleming, and Kenneth R. Pohl
Sandia National Laboratories, Albuquerque, NM, USA
kwojcie@sandia.gov

***Abstract*—It is well known that the stability of crystal oscillator references is undermined in high-g environments [1,2]. This can result in failure of communications systems relying on the crystal as a frequency reference. Lower vibration sensitivity is theoretically achievable by replacing the crystal with a micro electromechanical (MEMS) resonator. In this paper we present an electrostatically actuated Lamé resonator that has vibration sensitivity (0.91 ppb/g) comparable to the best high-g insensitive crystal oscillators.**

I. INTRODUCTION

This paper details the development of low vibration sensitivity bulk acoustic MEMS oscillators. Previous work that achieved a vibration sensitivity of ~7 ppb/g concentrated on the vibration sensitivity of Double Ended Tuning Fork (DETF) resonators with large gaps (~1um) [3]. Due to the large gaps, vibrations in the direction of oscillation had negligible effect on the DETF g-sensitivity and electrostatic spring softening could be ignored. However, in bulk acoustic devices spring softening cannot be ignored. Devices such as square extensional, Lamé, ring and disk resonators require narrow gaps to achieve acceptable motional impedances. When the nonlinearity of parallel plate actuators is accounted for, the effective stiffness of the resonator in the direction of oscillation (x) is given by (1).

$$k_{effective} \approx k_{m1} - k_{e1} + \left(k_{m3} - k_{e3}\right) \cdot x^2 \qquad (1)$$

Where k_{m1} and k_{m3} are the linear and third order mechanical spring constants and k_{e1} and k_{m3} are the linear and third order electrical spring constants. Due to the narrow gaps electrical spring constants dominates the vibration sensitivity of these devices.

Unfortunately, it is difficult to analytically determine the vibration sensitivity of the bulk acoustic resonators and it must be obtained through finite element modeling (FEM). Therefore, in this work we investigate how spring softening affects vibration sensitivity by examining a clamped-clamped (C-C) beam in Figure 1. This method was chosen for the modeling because they can be represented analytically using simple equations and are computationally inexpensive in FEM simulation, allowing rapid characterization of the vibration sensitivity over a number of design parameters. In addition, the conclusions drawn from this analysis can be directly applied to bulk acoustic resonator design. Finally we present the design of a low vibration sensitivity Lamé resonator followed by measurement results and conclusions.

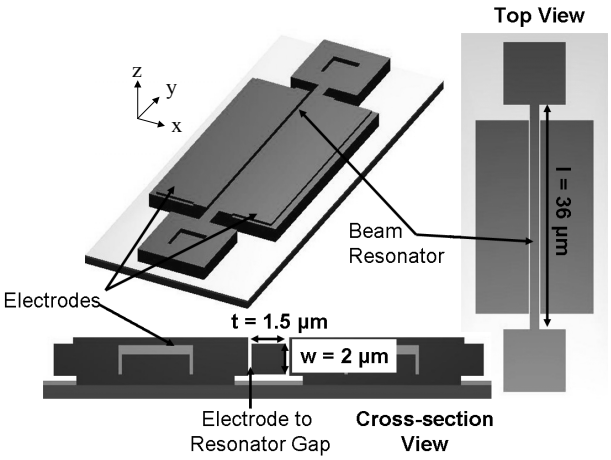

Figure 1: Diagram of clamped-clamped polysilicon beam used in vibration sensitivity analysis.

II. BEAM VIBRATION SENSITIVITY ANALYSIS

The underlying physical mechanisms that result in resonator vibration sensitivity (g-sensitivity) are due to nonlinearities that make the resonator stiffness dependent on its deflection. For instance mechanical spring nonlinearities (spring stiffening) can cause shifts in resonant frequency due to strain induced in the resonator by acceleration. In the case of electrostatic spring softening, accelerations in the direction of beam oscillation cause a mismatch in the gaps between the beam and the drive and sense electrodes. This mismatch reduces the effective stiffness of the resonator. In order to understand the effects of these mechanisms a clamped-clamped beam MEMS resonator with parallel plate capacitive actuators (Figure 1) was analyzed. This simplified model allows one to investigate how physical parameters such as resonator gap, bias voltage, electrode design and, resonator stiffness affect vibration sensitivity. The resonant frequency

This work was supported by the Laboratory Directed Research and Development (LDRD) program at Sandia National Laboratories. Sandia National Laboratories is a multiprogram laboratory operated by the Sandia Corporation, Lockheed Martin Company, for the United States Department of Energy's National Nuclear Security Administration under contract DE-AC04-94AL85000.

and g-sensitivity of the C-C polysilicon beam in Figure 1 can be modeled using the following set of equations (2-(8).

$$F_{total} = F_{acceleration} + F_{electrostatic} = 9.8 m_{beam} a + \frac{\varepsilon_0 A V_b^2}{2}\left[\frac{1}{(g_0 - z)^2} - \frac{1}{(g_0 + z)^2}\right] \quad (2)$$

$$z = \frac{F_{total}}{k_1 + k_3 z^2} \quad (3)$$

$$k_{m1} = \frac{\pi^4 E W_{beam} T_{beam}^{\ 3}}{6 L_{beam}^{\ 3}} \quad (4)$$

$$k_{m3} = \frac{\pi^4 E W_{beam} T_{beam}}{8 L_{beam}^{\ 3}} \quad (5)$$

$$k_{effective} = \frac{F_{acceleration}}{z} \quad (6)$$

$$f_{beam} = \frac{1}{2\pi}\sqrt{k_{effective} / m_{beam}} \quad (7)$$

$$\Gamma = \frac{f_{beam} - f_0}{f_0 a} \quad (8)$$

where m_{beam}, W_{beam}, T_{beam}, L_{beam}, and f_{beam} are the mass, width, thickness, length, and resonant frequency of the beam, V_b is the resonator bias voltage, A is the resonator/electrode overlap area, g_0 is the electrode to resonator gap, a is the acceleration in g applied normal to the direction of vibration, E is Young's modulus, f_0 is the resonant frequency with $a = 0$, and z is the maximum beam displacement, occurring at the center of the beam. In addition, k_1 and k_3 are the first and third order mechanical spring constants. Finally, Γ is the vibration sensitivity. In reality, the mass, spring constant, and displacement vary over the length of the beam [4] and equations 2-8 overestimate the vibration sensitivity because the entire beam is assumed to deflect by z, leading to an artificial increase in the electrostatic spring softening. Despite this inaccuracy, these equations are useful for predicting the effects of changing the beam geometry, gap, and bias voltage on the vibration sensitivity. Iterating equations 2-(3 and solving for the Γ results in a g-sensitivity 3.7 times higher than the FEM solution shown in Figure 2. Both the theoretical and FEM analysis predict (Γ is negative) that electrostatic spring softening, rather than spring stiffening, dominates the vibration sensitivity.

Due to the inaccuracies of equations 2-8 above and the increased complexity of the final high-g resonator design, finite element analysis was used to model resonator g-sensitivity. The g-sensitivity was modeled in ANSYS by: a) setting up a coupled mechanical/electrical analysis to simulate the spring softening effects, b) measuring the frequency with no applied g-load and, c) applying g-loads at 10 g, 100 g, 1 kilo-g , 10 kilo-g , and 100 kilo-g. The g-sensitivity of a 10 MHz polysilicon beam without an applied bias (no electrostatic spring softening) is $5x10^{-13}$/g at 100 kilo-g and is below the resolution of the FEM tool for accelerations below 100 kilo-g. The bias applied to the electrode, the electrode to resonator gap, and the configuration of the electrodes (differential vs. single ended) all significantly impact the g-sensitivity of the resonator. The g-sensitivity of the 10 MHz beam vs. g-load for a resonator with a differential drive and sense, a bias voltage of 12 V, and varied gap spacings is shown in Figure 2.

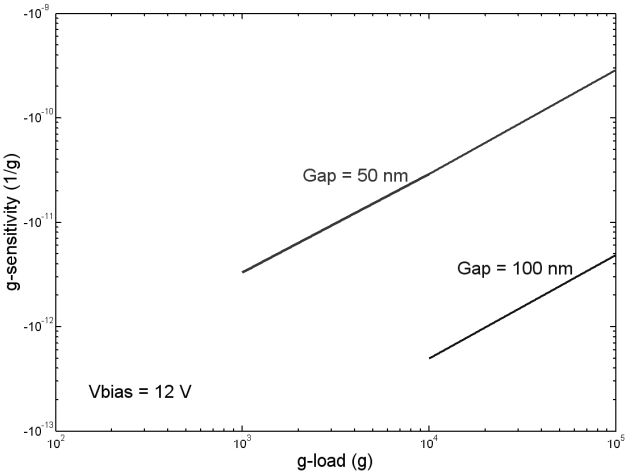

Figure 2: FEM simulated vibration sensitivity of a 10MHz clamped-clamped beam vs. electrode gap spacing.

The g-sensitivity of the same beam vs. g-load with a 100 nm electrode to resonator gap and varied bias voltages is shown in Figure 3. In Figure 2 and Figure 3, when no data is displayed at a certain g-load, no frequency shift is reported by ANSYS for that acceleration. When the electrostatic spring softening is included, Γ, becomes negative, increases in magnitude with increasing bias voltage and decreasing electrode/resonator gap. For a given acceleration it is possible, through proper choice of gap and bias voltage, to dramatically reduce the g-sensitivity by canceling the spring stiffening and softening. The electrode configuration also significantly impacts the g-sensitivity, as shown in Figure 4, where a differential drive/sense outperforms a single ended drive/sense by 2-3 orders of magnitude. Matching the gap spacing of the differential electrodes is also critical for achieving sub $1x10^{-11}$/g vibration sensitivity as shown in Figure 5. In order to significantly improve the vibration sensitivity over that of the best crystal oscillators ($1x10^{-10}$/g), MEMS resonators should operate at high frequency (> 10 MHz), have differential drive/sense electrodes with an electrode/resonator gap greater than 100 nm which can be matched within 1 nm.

III. Lamé Resonator Design and Process Flow

Using information derived from the 10 MHz polysilicon beam vibration sensitivity analysis, the 52 MHz, low g-sensitivity, Lamé resonator, shown in Figure 6, has been designed. The Lamé resonator was chosen due to the fact that it can be anchored in five locations. Hence, one can obtain high stiffness in all directions (low g-sensitivity) while still achieving high Q. The device is 67.5 μm square and it's supporting anchors beams are 4.5 μm long and 2 μm wide. The supporting beams were shortened from quarter wavelength to improve g-sensitivity. A cross-section of the 8-mask process is shown in Figure 7.

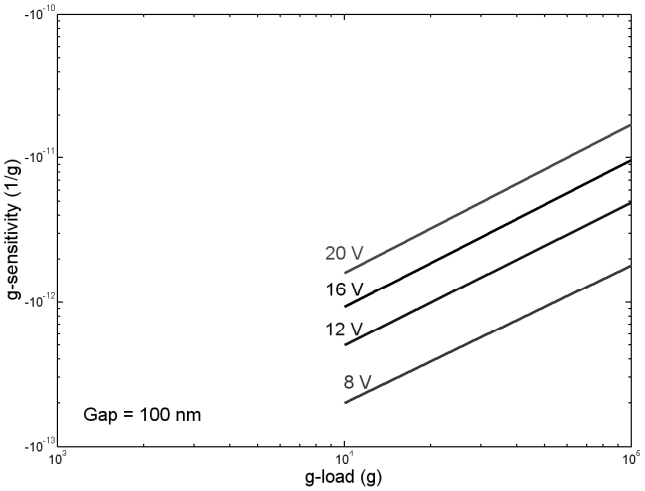

Figure 3: FEM simulated vibration sensitivity of a 10MHz C-C beam versus resonator bias voltage.

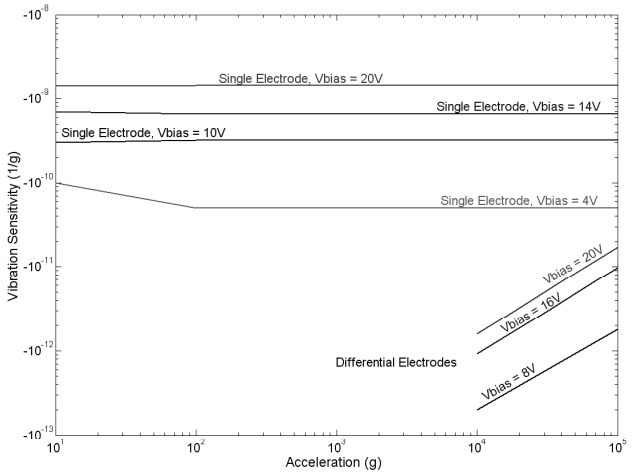

Figure 4: FEM simulated vibration sensitivity of single ended and differential electrodes for 10MHz C-C beam.

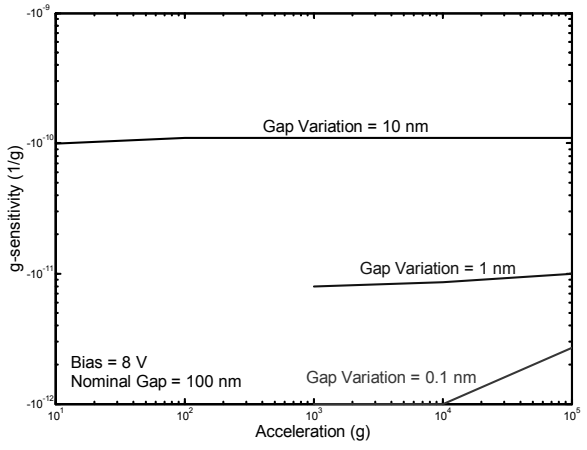

Figure 5: FEM simulated vibration sensitivity of differential 10MHz C-C beam versus offset between the two electrode/resonator gaps.

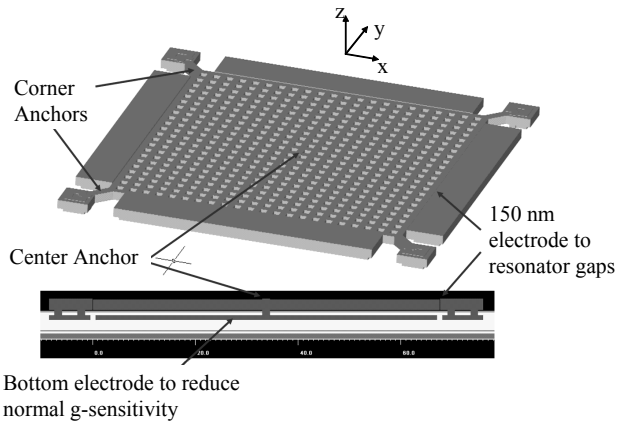

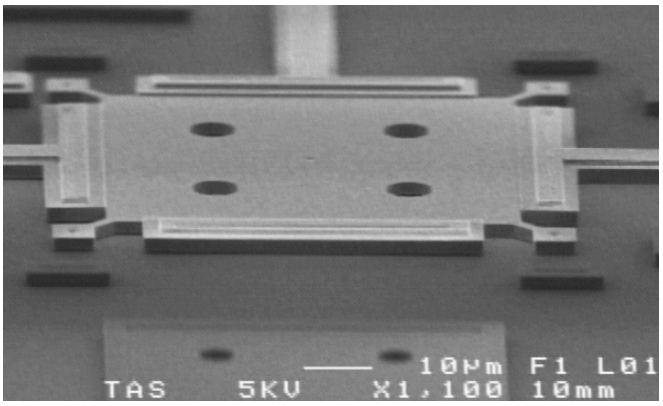

Figure 6: Lamé resonator diagram, cross-section and SEM.

The electrode/resonator gap is formed using an oxide spacer by Plasma-enhanced deposition of oxide from TEOS (PETEOS) followed by deposition of the electrode and release in buffered hydrofluoric acid (HF). The PETEOS 150nm oxide thickness is uniform to about two percent over a wafer and is expected to have much better than one percent matching in a single device. This is an important processing feature, as low g-sensitivity requires the matching of electrode gap to be better than 1 nm. Another key feature of the resonator design is the center anchor (the center anchor is not necessary for operation and slightly increases anchor losses), which reduces the g-sensitivity from accelerations normal to the substrate by several orders of magnitude. Including an electrode beneath the resonator tied to the resonator bias voltage not only prevents capacitive feed-through across the device, but also eliminates electrostatic spring softening due to accelerations normal to the substrate, further lowering the g-sensitivity. ANSYS simulations of the final Lamé resonator with an electrode to resonator gap of 150 nm and a bias voltage of 35V predict a g-sensitivity at 100 kilo-g of 4.2×10^{-3} ppb/g for accelerations normal to the substrate (z direction), and -4×10^{-6} ppb/g (at 100 kilo-g and 0.1% gap mismatch) for accelerations parallel (x dir) to the substrate. Frequency shifts for accelerations along the x axis are below the resolution of the FEM tool for accelerations less than100 kilo-g.

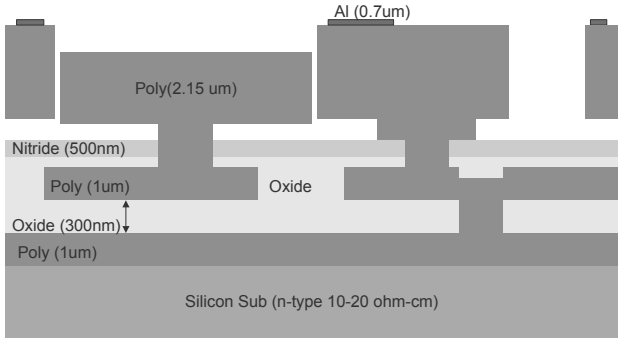

Figure 7: Cross-section after release of the high-g polysilicon resonator process.

A SEM image of the Lamé resonator is shown in Figure 6. The resonator is approximately 2.15 μm thick and has an electrode to resonator gap of 150 nm (This was the targeted gap spacing for the first devices). The transmission characteristic of a device similar to the one tested is shown in Figure 8.

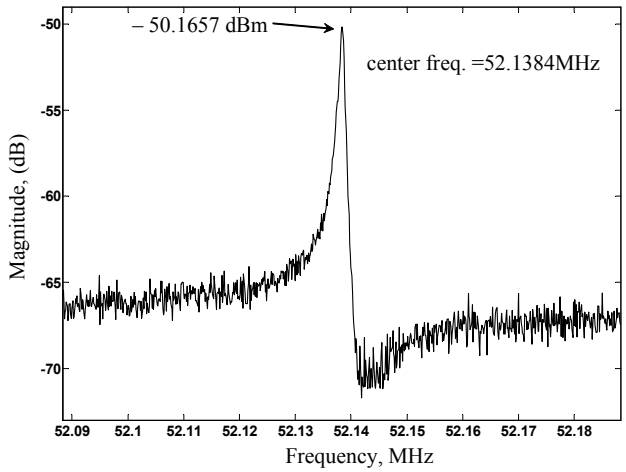

Figure 8: Measured Transmission characteristic of a 52 MHz Lamé resonator with 150 nm gaps measured in a chip scale vacuum package at 15V bias. The peak of the transmission spectrum is -50.17 dB. The Q is 52140 and motional impedance is 16 k**Ω.**

The actual device tested in this work was placed in a chip scale vacuum package. After packaging the resonator the resonators measured Q was 10,000. The measured motional impedance was 17 kΩ at a bias voltage of 35V.

IV. Oscillator Design and Experimental Results

The schematic diagram of the oscillator used in this work is shown in Figure 9. It is designed with three Phillips NE5211 transimpedance amplifiers (TIA). The first stage (part 0) provides a gain of approximately 14 kΩ [5]. The voltage gain of the second stage (part 1) is 14 kΩ/R1 = 14 and is adjustable by changing the values of R1. Finally R2 (1 kΩ) and R4 (200 Ω) form a voltage divider through which the maximum output voltage swing of the amplifier can be limited by adjusting R2 and R4. There was some concern that if the resonator were allowed to self-limit it would adversely affect the vibration sensitivity. As a result, this circuit was designed to provide a means of increasing gain while maintaining a desired maximum output swing through adjustment of the divider ratio and the gain of the second stage. However, for this device, it was discovered that the divider was not necessary. The power handling of the resonator was high enough that no self-limiting occurred when it was driven with maximum output voltage swing of the NE5211.

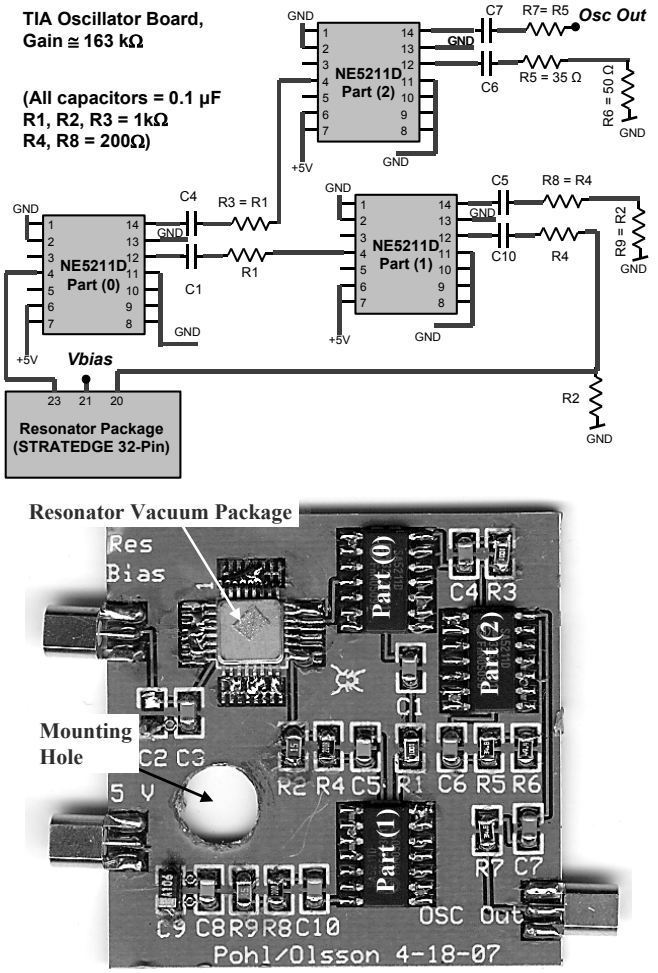

Figure 9: Schematic diagram of oscillator and PCB developed for testing of vibration sensitivity.

The printed circuit board (Figure 9) was mounted on a shaker table. Its velocity was measured optically using a Polytec OFV-552 vibrometer and OFV-5000 vibrometer controller. The device vibration sensitivity was measured in the x and z directions defined in Figure 6. Table 1 shows the results of the measurements. The worst-case sensitivity of 0.91 ppb/g was measured for vibrations in the z direction. An example of the output spectrum of the oscillator at rest (grey) and with a ~10g (sinusoidal) at 3 kHz in the x direction is shown in Figure 10. Note that the power of the oscillator output was measured to be –4.87 dBm. However because of the large span used in the spectrum analyzer measurement the peak power was not captured in the plot (Figure 10).

Table 1: Measured vibration sensitivity with a bias voltage of 35V

Vibration Direction	Vibration Amplitude (m/sec^2, peak to peak)	Vibration Frequency (kHz)	Sensitivity, $\lvert\Gamma\rvert$, ppb/g
X	77	0.6	0.21
X	75	3	0.28
X	102	3	0.71
Z	75	4	0.82
Z	79	10	0.91

The bias voltage of the resonator was varied in order to determine if the vibration sensitivity of the resonator is dominated by electrostatic nonlinearity. If so, sensitivity should be proportional to the square of the bias voltage applied to the resonator. Unfortunately the bias voltage could not be varied over a wide range. At biases less than 29V the oscillator ceased to operate. In addition, biases greater that 35V were avoided due to the possibility of pull-in. The results are shown in Figure 11. This data shows that the devices vibration sensitivity increases with resonator bias. This is consistent with the conclusion that the sensitivity is dominated by the spring softening.

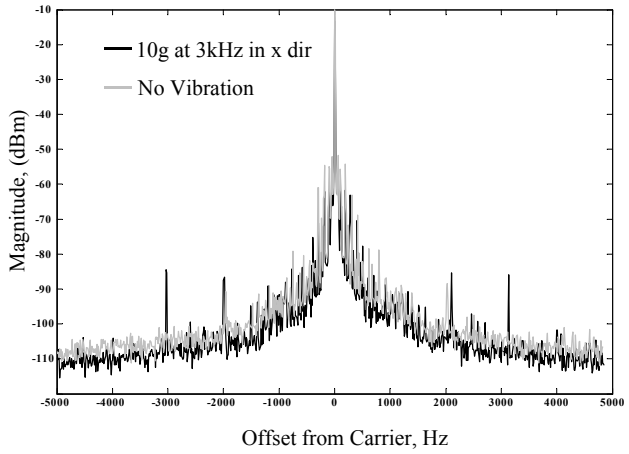

Figure 10: Oscillator Spectrum at rest (black) and spectrum with 10g at 3kHz applied in the x direction. Measured with a HP4396 spectrum/network analyzer.

V. CONCLUSIONS

Our first generation low g-sensitivity Lamé resonator achieved a maximum sensitivity of 0.91 ppb/g. This is commensurate with the performance of some of the best crystal oscillators (Statek HGXO and ECS-3951M crystal oscillators) and nearly an order of magnitude better than previously reported MEMS oscillator results [3]. The vibration sensitivity of the 20 MHz Statek HGXO oscillator was measured in our lab and found to be 0.46 ppb/g [6] for a peak sinusoidal acceleration of 19 g at 2 kHz. While our vibration sensitivities are comparable to the crystal, they are several orders of magnitude higher than that predicted by the FEM model. We are currently investigating several mechanisms that could be the cause of the discrepancy. They are: FEM modeling error, vibration modulation effects on cabling capacitance [7], and finally device anchor failure. The latter is perhaps the most plausible explanation. This is suspected for two reasons. First the resonators presented in this work have a known issue with undercutting of the anchor poly layer during HF release. Secondly, after the test at 10kHz (Table 1) a device failure occurred which caused the vibration sensitivity to increase dramatically (to 575 ppb/g). However there was no other observed change in oscillator performance. An anchor failure could be the possible cause since this type of failure would not cause the device to fail catastrophically. However, its vibration sensitivity would be severely compromised.

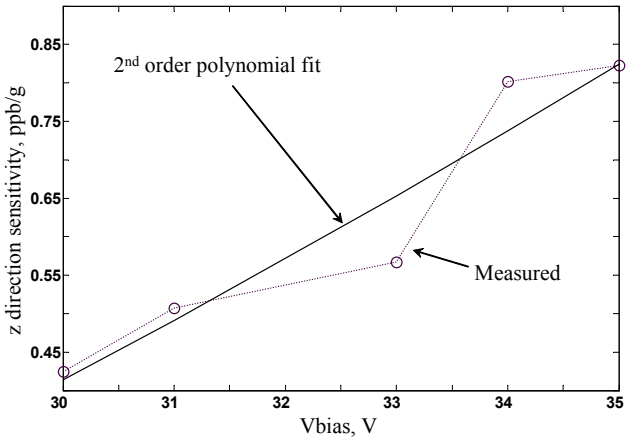

Figure 11: z direction vibration sensitivity versus bias voltage.

ACKNOWLEDGMENT

The authors would like to acknowledge the staff of the Microelectronics Development Laboratory (MDL) for their help in the development of the resonator fabrication process. We would also like to thank David Epp of Sandia National Laboratories for his assistance with the vibrometer testing.

REFERENCES

[1] Kosinski, J. A., "Theory and design of crystal oscillators immune to acceleration: Present state of the art," 2000 IEEE/EIA international frequency control symposium and exhibition, pp. 260-268.

[2] Filler, R. L., "The acceleration sensitivity of quartz crystal oscillators: A review," IEEE Trans. on ultrasonics, ferroelectrics, and frequency control, vol. 35, no. 3, May 1988, pp. 297-305.

[3] Agarwal M., et.al., "Effects of mechanical vibrations and bias voltage noise on phase noise of MEMS resonator based oscillators," 19th IEEE international conference on micro electro mechanical systems, Istanbul, Turkey, 2006, pp. 154-157

[4] Bannon III, F. D., Clark, J. R., and Nguyen, C. T.-C., "High-Q HF micromechanical filters," IEEE Journal of Solid-State Circuits, vol. 35, no. 4, April 2000, pp. 512-526.

[5] NE5211 180MHz Transimpedance Amplifier Data sheet.

[6] Olsson III, R. H., "SAND2005-7520: Low Vibration Sensitivity MEMS Oscillators for RF Data Transmission During High-G Penetration Events." Unpublished Sandia National Laboratories internal memo. November, 2005.

[7] Hanson, W. P., et.al., "A new factor affecting the acceleration sensitivity of the resonance frequency of quartz crystal resonators," Proceedings of 44th IEEE international frequency control symposium, 1990, pp. 478-492